













## Distribution of nesfatin-1 expression in Bactrian camels and its impact on adipocyte glucose metabolism<sup>1</sup>

Siriguleng Yu<sup>2\*</sup> , Bijun Chen<sup>2</sup> , Haoyu Bai<sup>2</sup> , Ziyi Li<sup>2</sup> , Yaru Niu<sup>2</sup> ,  
Xingchuan He<sup>2</sup> , Wen Yu<sup>2</sup> , Shumin Du<sup>2</sup> , Junjian Jin<sup>2</sup>   
and Hongqiang Yao<sup>2,3,4</sup> 

**ABSTRACT.** Yu S., Chen B.J., Bai H.Y., Ai D., Li Z.Y., Niu Y.R., He X.C., Yu W., Du S.M. Jin J.J. & Yao H.Q. 2024. **Distribution of nesfatin-1 expression in Bactrian camels and its impact on adipocyte glucose metabolism.** *Pesquisa Veterinária Brasileira* 44:e, 2024. Key Laboratory of Clinical Diagnosis and Treatment Technology for Animal Diseases, Ministry of Agriculture, College of Veterinary Medicine, Inner Mongolia Agricultural University, Hohhot, Inner Mongolia 010020, China. E-mail: [srglyu@imau.edu.cn](mailto:srglyu@imau.edu.cn)

The study aimed to investigate the distribution and expression of nesfatin-1 in Bactrian camels and its impact on adipocyte glucose metabolism. Polyclonal antibodies against a single antigenic epitope of NUCB2/nesfatin-1 protein were prepared. Nesfatin-1 expression was detected in various adipose tissues, including the hypothalamus, humps, stomach, duodenum, jejunum, ileum, cecum, colon, rectum, pancreas, liver, and abdomen, using Western blot and qRT-PCR. Glucose uptake levels, pyruvic acid content, and hexokinase and phosphofructokinase activities were measured in cultured 3T3-L1 preadipocytes treated with nesfatin-1 in a high glucose state using a non-radiofluorimetric assay. The results showed that nesfatin-1 was found in all Bactrian camel tissues, with higher adipose tissue and pancreas expression. However, qRT-PCR analysis revealed higher expression of nesfatin-1 mRNA in the abdominal fat and liver. After nesfatin-1 treatment, a significant decrease ( $p < 0.05$ ) was observed in glucose uptake levels, hexokinase, and phosphofructokinase activities in 3T3-L1 cells, with a significant increase ( $p < 0.05$ ) in their pyruvic acid content. These findings suggest that nesfatin-1 is expressed at high levels in the abdominal fat of Bactrian camels and significantly affects adipocyte glucose metabolism by regulating blood glucose levels, inhibiting adipocyte differentiation, and promoting lipid droplet hydrolysis to provide energy for the organism, which may relate to the Bactrian camel's ability to adapt to harsh environments.

INDEX TERMS: Bactrian camel, nesfatin-1, polyclonal antibody, adipocyte, glucose metabolism.

### INTRODUCTION

Nesfatin-1 is generated through the hydrolysis of NUCB2 (Dore et al. 2017) and plays a role in appetite regulation and glycolipid metabolism (Oh-I et al. 2006). It affects energy metabolism and can regulate glucose-sensing neurons, impacting blood glucose levels and food intake (Shimizu et al. 2009, Chen et al. 2012, Gantulga et al. 2012, Dong et al. 2014). Nesfatin-1 also modulates protein kinase B (AKT) phosphorylation and glucose transporter

protein 4 (GLUT 4) membrane translocation, leading to increased insulin secretion and improved insulin sensitivity, thus regulating glucose metabolism (Li et al. 2013). Yang et al. (2019) research also indicates that pancreatic beta-cells synthesize NUCB2/nesfatin-1 proteins, influencing glucose-stimulated insulin secretion and insulin sensitivity. Additionally, nesfatin-1 promotes free fatty acid oxidation in skeletal muscle through specific pathways (Dong et al. 2013) and lipid hydrolysis for energy supply (Tagaya et al. 2012, Lim et al. 2020).

As we all know, nesfatin-1 is widely distributed in the central and peripheral tissues of the organism, influencing energy metabolism and appetite regulation. However, its distribution and function in the Bactrian camels are not yet clear. In this study, we developed a polyclonal antibody against nesfatin-1 to investigate its expression and detected its impact on energy metabolism in Bactrian camels. The aim was to lay the groundwork for future research on the

<sup>1</sup> Received on May 26, 2024.

Accepted for publication on June 23, 2024.

<sup>2</sup> Key Laboratory of Clinical Diagnosis and Treatment Technology for Animal Diseases, Ministry of Agriculture, College of Veterinary Medicine, Inner Mongolia Agricultural University, Hohhot, Inner Mongolia 010020, China. \*Corresponding author: [srglyu@imau.edu.cn](mailto:srglyu@imau.edu.cn)

<sup>3</sup> Inner Mongolia Camel Protection Association, Hohhot 010018, China.

<sup>4</sup> China Camel Industry Association, Beijing 100044, China.

relationship between nesfatin-1 and the regulation of obesity and blood glucose, potentially providing insights into the prevention and treatment of obesity and metabolic diseases.

## MATERIALS AND METHODS

**Animal Ethics.** The research protocols were approved by the Experimental Animal Welfare and Ethics Committee of Inner Mongolia Agricultural University (No. NND2021034) on March 9, 2021.

**Animals, tissues and cells.** Vaccinated New Zealand purebred large white rabbits (New Zealand rabbits, New Zealand, healthy males, 4~5 months old, weighing about 2.5kg) were purchased from Beijing Changyang Xishan Breeding Farm. Tissue samples were collected from Bactrian camels (n=7) in Shibatai Township, Zhuozishan Town, Wulanchabu, Inner Mongolia. Mouse preadipose embryonic fibroblasts (3T3-L1 cell line) were purchased from Green Flag Bio-Technology Development Co., Ltd (Shanghai, China).

**Design of nesfatin-1 epitope peptides.** The protein sequence XP\_010963104.1 of the Bactrian camel's NUCB2 was chosen from NCBI and analyzed by DNASTar software. Based on the secondary structure analysis of the protein sequence, as well as considerations of hydrophilicity and antigenicity, antigenic epitope polypeptide fragments were carefully selected. After the analysis, the antigenic sequences that exhibited superior specificity, antigenicity, and hydrophilicity were pinpointed within amino acids 1 to 82. The chosen amino acid sequence was Pep: C\*ETDSHFREKLQKAD, where C\* (cysteine) is artificially added (Li et al. 2018) for facilitating subsequent coupling with keyhole limpet hemocyanin (KLH) and bovine serum albumin (BSA) to form complete antigens. This process involved partnering with KLH to create immunoantigens and with BSA to create encapsulated antigens.

**Peptides coupled to keyhole limpet hemocyanin (KLH) and bovine serum albumin (BSA).** The specific epitope peptide of the Bactrian camel nesfatin-1 protein was chemically synthesized and subsequently conjugated to keyhole limpet hemocyanin (KLH) and bovine serum albumin (BSA) utilizing the maleimide method. The success of the coupling process was assessed using the Ellman reagent method. The efficiency of peptide coupling with KLH and BSA was evaluated by determining the cysteine (Cys) content. Prior to the experiment, a cysteine standard curve was generated using a standard cysteine, and the samples' cysteine concentrations were measured and plotted against the standard curve to gauge the change in cysteine concentration before and after the coupling process. This approach allowed for calculating the peptide coupling rate with KLH and BSA.

The formula for determining the coupling rate is as follows: Coupling rate =  $(1 - \text{cysteine concentration of the sample after coupling} / \text{cysteine concentration of the sample before coupling}) \times 100\%$ .

Production of polyclonal antibodies. Blood was obtained from the earlobe vein of New Zealand White rabbits before immunization to collect serum for use as the negative control. The immunogen was dissolved in sterile saline and used for the initial immunization, which was carried out by administering a complete antigen emulsion with Freund's Complete Adjuvant (Sigma-Aldrich, USA) at four different subcutaneous injection sites on the backs of the New Zealand white rabbits, with a dosage of 500 $\mu$ L at each site.

The first booster immunization was administered three weeks later, with the peptide fully emulsified in Freund's incomplete adjuvant (Sigma-Aldrich, USA) at four different subcutaneous injection sites. Subsequent booster immunizations were given after five and seven weeks, and blood was drawn from an earmargin vein 10 days after the final booster immunization. The potency of the polyclonal

antibodies present in the serum was subsequently evaluated using an indirect enzyme-linked immunoassay.

**Purification and characterization of polyclonal antibodies.** A 2mL of SulfoLink coupling resin was introduced into the affinity column, and 5mg of the peptide was added to couple with the affinity resin column. Next, the antiserum was centrifuged at 4°C to eliminate any particles or erythrocytes and then diluted at a 1:1 ratio in phosphate-buffered saline (PBS). Affinity purification of the antisera was carried out using an affinity column, resulting in the eluate containing the polyclonal antibody. The eluate was concentrated to a level of 1-2g/L using ultrafiltration tubes (with a molecular weight cutoff of 10ku) before being mixed with 30%-50% glycerol and stored at -20°C.

For the preparation of colloids, the SDS-PAGE gel preparation kit was utilized to create 12% separating gels and 5% concentrated gels based on the molecular weight size of the target protein. The purified polyclonal antibody was adjusted to the appropriate concentration, and a quarter volume of protein loading buffer was added. Protein denaturation was achieved using a metal bath at 100°C for 5 min, followed by rapid cooling in an ice bath and subsequent centrifugation at 1,000rpm for 2 min. Polyacrylamide gel electrophoresis (SDS-PAGE) was performed with a 5% concentrate gel and a 12% separating gel. After electrophoresis, the gel was removed and placed in an imaging device for development imaging.

**Western blot.** The protein concentration in various Bactrian camel tissues was determined using the BCA kit (Beijing Solarbio Science & Technology Co., Ltd., China). Proteins were separated using 10% SDS-PAGE separating gel and 5% concentrate gel and then transferred to PVDF membranes via semi-dry transfer. Following sealing with 5% nonfat dry milk for 3 hours, the membranes were incubated with the aforementioned purified polyclonal antibody at 4°C overnight, followed by five washes with TBST for 10 min each. Subsequently, the membrane was incubated with horseradish peroxidase-conjugated goat anti-rabbit antibody (Sangong Biological Engineering Co., Ltd., Shanghai, China) for 1 hour at room temperature and then washed five times with TBST for 10 min each. The strips were developed and imaged using the ECL Luminescent Chromogenic Kit (Thermo Fisher Scientific, China), and the final images were compared using optical density analysis with ImageJ analysis software.

**RNA extraction and quantitative real-time PCR (qRT-PCR).** RNA was extracted from Bactrian camel tissues in accordance with the instructions of Axygen Scientific's total RNA extraction kit. The RNA was reverse transcribed into cDNA and stored at -80°C following the instructions of Takara's reverse transcription kit. The qRT-PCR assay was performed using pre-synthesized primers for the corresponding genes (NUCB2/nesfatin-1,  $\beta$ -actin), with  $\beta$ -actin as the internal reference gene. Data statistics and analysis were conducted on the completed assay results using a qRT-PCR instrument. The primer sequences were synthesized by Sangong Biological Engineering Co., Ltd., Shanghai, China – NUCB2-pF: 5'TCG AGA GCC TGT TAA GAA TCA GC 3', NUCB2-pR: 5'AGT ATG GTC CTC CAC TTC ATC TTT 3'.  $\beta$ -actin-pF: 5'GGA CTT CGA GCA GGA GAT GG 3',  $\beta$ -actin-pR: 5'AGG AAG GAG GGC TGG AAG AG 3'.

**Cell culture and differentiation.** 3T3-L1 preadipocytes were cultured in a 6-well plate and maintained in a complete medium, Dulbecco's modified eagle medium (DMEM) with higher glucose levels (Gibco, China) supplemented with 10% FBS and 1% P/S at 37°C in 5% CO<sub>2</sub>. The cells were grown to 100% confluence in a complete medium. The complete medium contained 2 $\mu$ g/mL dexamethasone, 0.5mM IBMX, and 10 $\mu$ g/mL insulin was added at day 0 to induce differentiation. After two days of induction, the medium was replaced

with a complete medium containing 10 µg/mL of insulin. Following an additional two days (day 4), the medium was changed to fresh medium for another four days. After eight days, cells were fully differentiated into adipocytes.

**Oil red O staining.** After differentiation, the adipocytes were fixed with 4% formalin and incubated at room temperature for at least 1 hour. After fixation, cells were washed twice with purified water and then washed with 60% isopropanol at room temperature for 5 min. The cells were dried completely at room temperature, and oil red O solution was added and then incubated at room temperature for 10 min. Oil red O solution was removed by adding purified water, and the cells were washed four times with purified water. Images were acquired using a microscope.

**Mensuration of glucose uptake levels.** The 3T3-L1 adipocytes were randomly divided into control and test groups. The test group was treated with high-sugar DMEM cell culture medium, and according to the reference method (Riva et al. 2011), the cells were treated with 100 nmol nesfatin-1 for 1 hour, while the control group was treated with the same amount of saline. After incubating with 1 mmol 2-deoxyglucose (2DG) for 10 min at room temperature, termination buffer, neutralization buffer, and 2-deoxyglucose-6-phosphate (2-DG6P) was added, and glucose uptake was detected using a multifunctional enzyme marker.

**Mensuration of pyruvic acid.** Before measuring the pyruvic acid content of the samples, a standard curve was generated using standards. The samples were then analyzed for pyruvic acid content. Following the nesfatin-1 intervention, 3T3-L1 adipocytes from the control and test groups were centrifuged to remove the supernatant. Subsequently, they were ultrasonically disrupted using a cell volume ratio of 104:500-1,000 (ultrasonication for 3 s, with an interval of 10 s, repeated 30 times) and then allowed to stand for 30 min. The supernatant was collected after centrifugation for 10 min at 8,000g and used for assay. Following the protocol of the pyruvic acid content assay kit (Beijing Solebao Technology Co., Ltd., China), the standards were diluted with distilled water to achieve concentrations of 25, 12.5, 6.25, 3.125, 1.5625, 0.78125, and 0 µg/mL. Subsequently, 75 µL of standard or sample and 25 µL of reagent I were added to a 96-well plate, mixed thoroughly, and allowed to stand for 2 min. Then, 125 µL of reagent II was added, mixed well, and the sample was examined in the 96-well plate for 2 min. Finally, 125 µL of reagent II was added and mixed well, and the absorbance value was measured at 520 nm.

**Measurement of hexokinase and phosphofructokinase activities.** The cells that received ultrasonic treatment were centrifuged, and the resulting supernatant was used for measurement following the previously described method. The instructions of the Hexokinase and Phosphofructokinase Activity Assay Kit (Beijing Solarbio Science & Technology Co., Ltd., China) were followed. According to the assay kit's instructions, 180 µL and 170 µL of reagent II, 10 µL of reagent III and 10 µL of reagent IV, as well as 10 µL of samples, were added to the 96-well plate. The absorbance values at 340 nm were immediately recorded for 20 seconds after mixing. Subsequently, the absorbance value at 340 nm for 20 seconds was recorded after placing the reaction in a 37°C thermostat for 5 min.

**Statistics and analysis.** Statistical analysis was conducted using GraphPad Prism 5.0 software. Experimental data were expressed as mean ± standard deviation and analyzed using the t-test. The value  $p < 0.01$  indicates a highly significant difference,  $p < 0.05$  indicates a significant difference, and  $p \geq 0.05$  indicates an insignificant difference. The qRT-PCR results were processed using the  $2^{-\Delta\Delta Ct}$  method.

## RESULTS

### Screening for nesfatin-1 epitope peptides

The amino acid sequence of XP\_010963104.1 was analyzed, and the antigenic sequence pep3:C\*ETDSHFREKLQKAD, with superior specificity, antigenicity and hydrophilicity, was selected as the antigenic epitope polypeptide fragment (Fig.1).

### Characterization of the effect of peptide coupling at the nesfatin-1 epitope

A standard curve was plotted using cysteine standards to determine the concentration of cysteine (Fig.2). The coupling rate of polypeptides with specific epitopes of Bactrian camel NUCB2/nesfatin-1 protein to KLH was calculated to be 84.1%, and the coupling rate BSA was calculated to be 77.9%. Results indicated that the peptide with a specific epitope of Bactrian camel NUCB2/nesfatin-1 protein was ideally coupled with carrier proteins (KLH and BSA) and could be used as an immunogen and coating antigen.

### Mensuration of polyclonal antibody potency

Indirect enzyme-linked immunosorbent assay (ELISA) was used to determine the potency of the polyclonal antibodies, and the calculated potency was greater than  $5.12 \times 10^5$  (Fig.3).

### Affinity purification of polyclonal antibodies

After affinity purification, the polyclonal antibody was denatured in a metal bath, leading to the emergence of the target bands during SDS-PAGE electrophoresis (Fig.4).

### Expression and distribution of NUCB2/nesfatin-1 protein in 15 tissues of Bactrian camel

Immunoblot analysis was conducted on sera from seven Bactrian camels. Positive bands appeared at 55 kDa in all seven Bactrian camels, consistent with the expected size of the target NUCB2/nesfatin-1 protein (47.5-55 kDa), indicating that the prepared polyclonal antibody could specifically recognize the NUCB2/nesfatin-1 protein in Bactrian camels (Fig.5). The expression of NUCB2/nesfatin-1 protein was examined in various tissues from Bactrian camels. The analysis revealed higher expression of NUCB2/nesfatin-1 protein in hump fat and lower expression in abdominal fat, pancreas, liver, arcuate nucleus, solitary tract nucleus, and medial ventral nucleus (Fig.6, column a). Additionally, NUCB2/nesfatin-1 protein expression in Bactrian camels exhibited higher levels in fore hump fat, jejunum, and pancreas. At the same time, it showed lower expression in abdominal fat, colon, rectum, liver, arcuate nucleus, solitary tract nucleus, and medial ventral nucleus (Fig.6, column b). Furthermore, the NUCB2/nesfatin-1 protein in Bactrian camels demonstrated higher expression in hump fat, abdominal fat, duodenum, jejunum, and pancreas, and lower expression in the cecum, liver, solitary tract nucleus, and medial ventral nucleus (Fig.6, column c). Collectively, these findings suggest that the NUCB2/nesfatin-1 protein in Bactrian camels has higher expression in fat tissues and lower expression in the liver, solitary tract nucleus and medial ventral nucleus.

### Expression levels of NUCB2/nesfatin-1 mRNA in 15 tissues of the Bactrian camel

The relative expression of Bactrian camel NUCB2/nesfatin-1 mRNA was high in different tissue samples. In Figure 7, column a, the mRNA showed high expression in abdominal fat, liver,

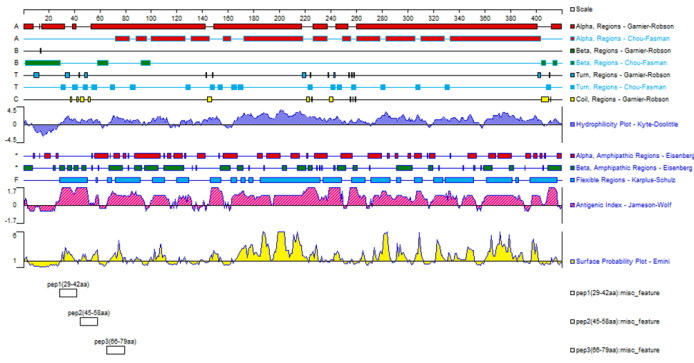


and medial ventral nucleus. Similarly, in Figure 7, column b, the mRNA exhibited high expression in antral fat, abdominal fat, stomach, and liver. Furthermore, in Figure 7, column c, the mRNA was seen to have high expression in abdominal fat and liver. These results collectively indicate that Bactrian camel NUCB2/nesfatin-1 mRNA is highly expressed in abdominal fat and liver.

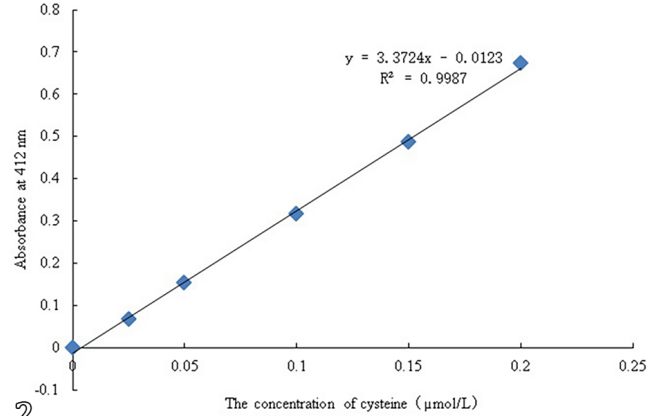
**3T3-L1 preadipocytes stained with Oil red O**

Under the light microscope, the 3T3-L1 preadipocytes' morphology resembles that of fibroblasts, displaying a long

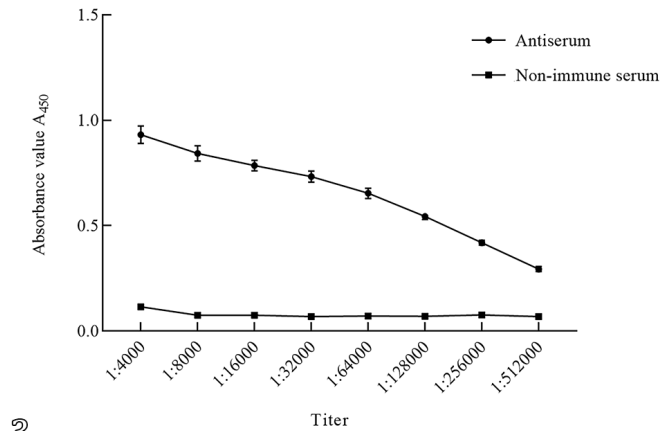
pike shape and no intracellular lipid accumulation. Notably, no staining is detected after Oil red O staining (Fig.8). After differentiation induction, it becomes evident that the cell morphology becomes more rounded, with lipid droplets appearing in the cytoplasm. Throughout the differentiation process, the accumulation of lipid droplets progressively increases. After eight days of induced differentiation, over 90% of the cells exhibited an adipocyte phenotype, with a substantial number of lipid droplets accumulated in the cytoplasm. The cells also display post-Oil red O staining (Fig.9).



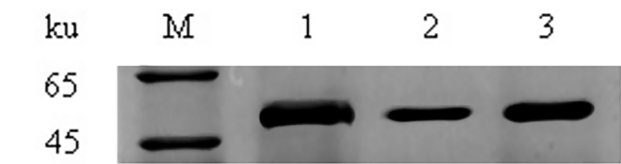
1



2

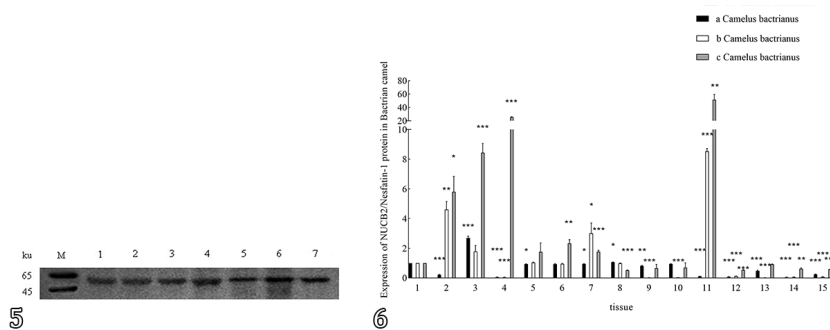


3



4

Fig.1-4. Production of polyclonal antibody. (1) Screening for nesfatin-1 epitope peptides. (2) Evaluation of peptide coupling efficiency. (3) Assessment of polyclonal antibody potency. (4) Affinity purification of polyclonal antibodies. Hohhot/NM, 2021.



5

Fig.5-7. Expression and distribution of NUCB2/nesfatin-1 in 15 tissues of the Bactrian camel. (5) Western blot analysis of seven camels. (6) Expression and distribution of NUCB2/nesfatin-1 protein in 15 tissues of bactrian camel. (7) Expression levels of NUCB2/nesfatin-1 mRNA in 15 tissues of bactrian camel. Hohhot/NM, 2021.

### Effect of nesfatin-1 on glucose uptake in 3T3-L1 preadipocytes

Cellular energy for organism activities is provided through glucose uptake. The outcomes indicate a highly significant reduction ( $p < 0.01$ ) in glucose uptake levels of adipocytes in the test group following nesfatin-1 intervention compared to the control group (Fig.10), signifying a notable decrease in sugar consumption by 3T3-L1 adipocytes.

### Effect of nesfatin-1 on pyruvic acid content of 3T3-L1 preadipocytes

Before analyzing and determining the pyruvic acid content of the samples, gradient diluted standards were first assayed

using an enzyme marker to establish a pyruvic acid detection standard curve. The standard curve of the pyruvic acid content of the standard was  $y = 0.0257x + 0.0819$ ,  $R^2 = 0.9997$ , consistent with the assay standard (Fig.11). There was no significant difference in the pyruvic acid content of 3T3-L1 adipocytes between the control and test groups ( $p > 0.05$ ) (Fig.12).

### Effect of nesfatin-1 on hexokinase activity in 3T3-L1 preadipocytes

Hexokinase is a crucial enzyme in glucose breakdown, catalyzing the conversion of glucose to glucose-6-phosphate, a pivotal step in glycolysis and pentose phosphate pathways.

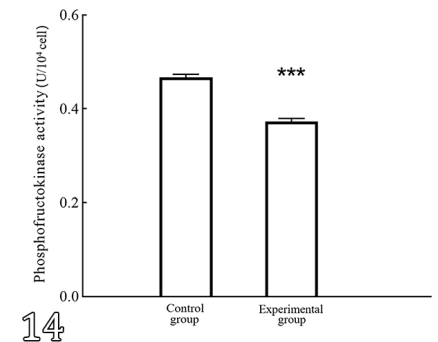
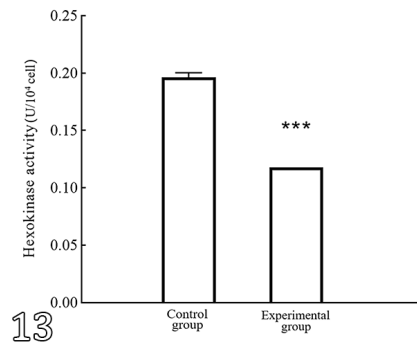
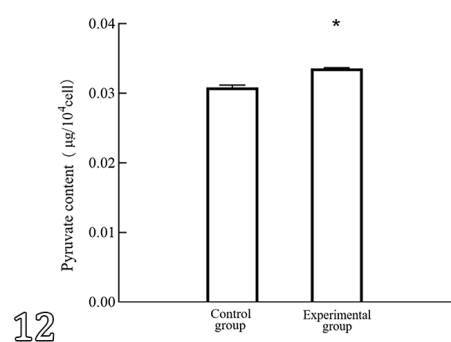
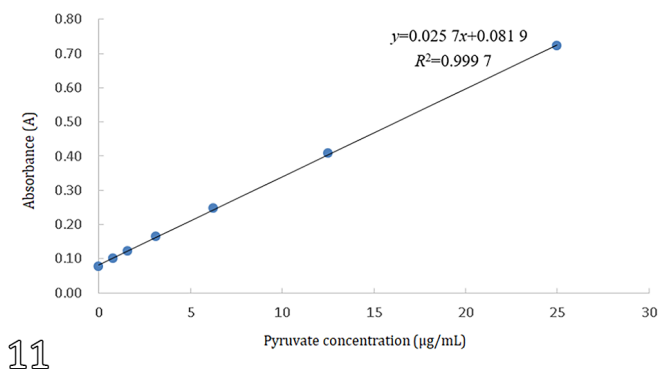
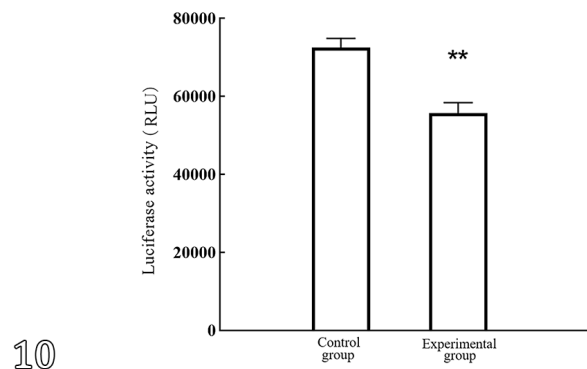
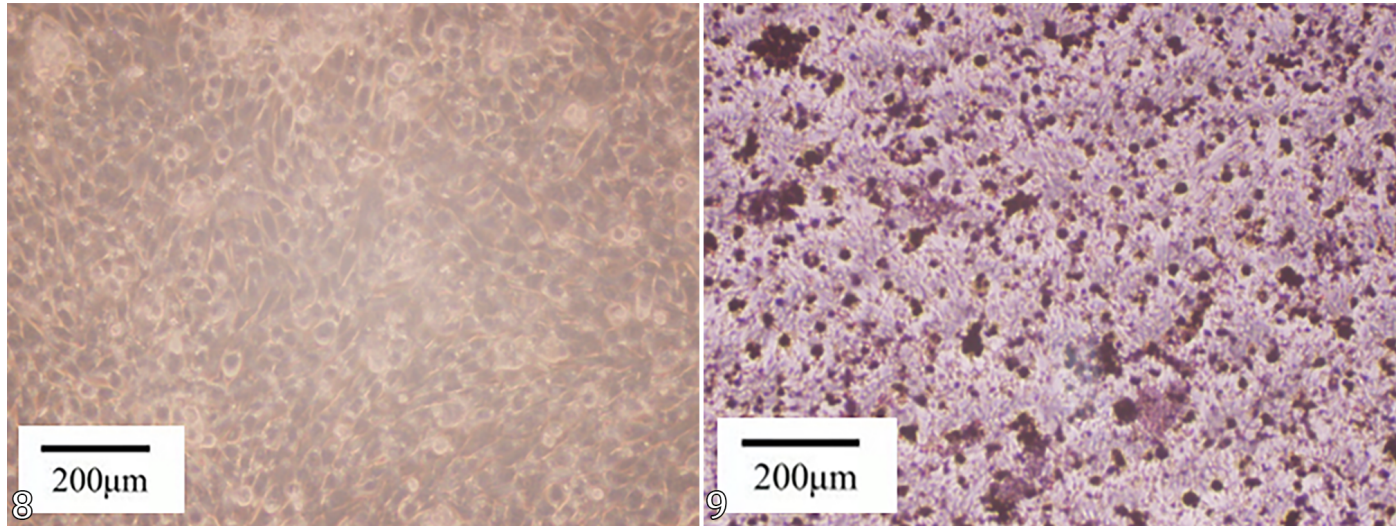


Fig.8-14. Effects of nesfatin-1 on 3T3-L1 preadipocytes under high glucose conditions. (8-9) Microscopic images of 3T3-L1 preadipocytes before and after staining with Oil red O. 3T3-L1 adipocytes. Oil Red O, obj.40x. (10) Impact of nesfatin-1 on glucose uptake levels in 3T3-L1 preadipocytes. (11-12) Influence of nesfatin-1 on pyruvic acid content of 3T3-L1 preadipocytes. (13) Effect of nesfatin-1 on hexokinase activity in 3T3-L1 preadipocytes. (14) Effect of nesfatin-1 on phosphofructokinase activity in 3T3-L1 preadipocytes. Hohhot/NM, 2021.

Results demonstrate a substantial reduction in hexokinase activity in 3T3-L1 adipocytes in the test group compared to the control group ( $p < 0.001$ ) (Fig.13).

### Effect of nesfatin-1 on phosphofructokinase activity in 3T3-L1 preadipocytes

Phosphofructokinases are enzymes that catalyze a crucial irreversible reaction in glucose metabolism. Phosphofructokinase activity was markedly decreased in 3T3-L1 adipocytes in the test group compared to the control group ( $p < 0.001$ ) (Fig.14).

## DISCUSSION

The exceptional metabolic abilities of the Bactrian camel, including its remarkable endurance to thirst and hunger and adaptation to challenging environments, strongly suggest a correlation with metabolic regulation. Nevertheless, the specific involvement of nesfatin-1 in these processes remains unclear. Therefore, the primary objective of this study is to analyze the distribution of nesfatin-1 in Bactrian camels and elucidate its potential impact on their metabolic processes. Our study successfully generated polyclonal antibodies targeting a specific antigenic epitope of the Bactrian camel NUCB2/nesfatin-1 protein through peptide synthesis. Then we observed higher expression of NUCB2/nesfatin-1 in hump fat and abdominal fat of Bactrian camels, similar to findings in rodent and human adipose tissues (Ramanjaneya et al. 2010). Prior research has illustrated its involvement in modulating energy metabolism and its link to obesity, diabetes mellitus, and cardiovascular disease (Li et al. 2010, Zhang et al. 2012, 2017a, Ramesh et al. 2017, Yang et al. 2017). As a result, these findings suggest a pivotal role for nesfatin-1 in metabolic regulation within the Bactrian camel.

Tagaya et al. (2012) identified a novel physiological function of NUCB2/nesfatin-1, which inhibits adipocyte differentiation (Tagaya et al. 2012). This specific function of nesfatin-1 may be linked to the ability of the Bactrian camel to adapt to severe environments. In such environments, the stored fat in the hump and abdomen could supply the energy needed for the camel to survive, thus aiding in its adaptation to harsh conditions. Moreover, NUCB2/nesfatin-1 has been identified as a pro-insulin peptide, facilitating insulin secretion in high glucose environments (Gonzalez et al. 2011). Previous research has shown the presence of NUCB2/nesfatin-1 proteins in rat/mouse islets and their secretion in pancreatic islets (Foo et al. 2010). Therefore, drawing on our experimental findings, we hypothesize that NUCB2/nesfatin-1 proteins may play a significant role in insulin secretion, thereby regulating blood glucose levels and maintaining homeostasis in Bactrian camels.

In order to further investigate the role of nesfatin-1 in metabolic regulation, the study attempted to simulate the hyperglycemic environment of a Bactrian camel. It examined nesfatin-1's impact on adipocyte glucose metabolism in high glucose conditions. Under normal conditions, cellular glucose metabolism primarily involves processes such as glucose uptake, glycolysis leading to pyruvate formation, and various other enzymatic activities, ultimately resulting in the synthesis of large amounts of ATP to provide energy for the cell's metabolic activities (Boussouar & Benahmed 2004). However, this study observed a significant reduction in glucose uptake by 3T3-L1 adipocytes under high-glucose conditions following nesfatin-1 intervention. Moreover, the

intracellular activities of hexokinase and phosphofructokinase were also significantly diminished, indicating a potential shift in the metabolic pathways of the adipocytes. The findings align with the role of nesfatin-1 in promoting adipocyte catabolism (Zhang et al. 2017b). These results indicate that nesfatin-1 can effectively reduce the glucose consumption of 3T3-L1 adipocytes and warrant further investigation into its underlying mechanisms.

## CONCLUSIONS

A polyclonal antibody targeting the Bactrian camel NUCB2/nesfatin-1 protein was successfully generated by conjugating the protein's specific epitope peptide with a carrier protein. Notably, the expression of both nesfatin-1 protein and mRNA was significantly higher in the adipose tissue of Bactrian camels. Furthermore, under high glucose conditions, adipocytes may experience reduced glucose uptake and decreased activity of intracellular enzymes involved in glucose metabolism in response to nesfatin-1.

The higher expression of nesfatin-1 in the adipose tissue of Bactrian camels may play a vital role in regulating blood glucose levels, inhibiting adipocyte differentiation, and promoting lipid droplet hydrolysis to provide energy, all of which may potentially contribute to the Bactrian camel's ability to adapt to harsh environments.

**Authors' contributions.**- The authors Siriguleng Yu and Bijun Chen contributed equally to the work and should be regarded as co-first authors. Siriguleng Yu and Hongqiang Yao conceived and guided the whole project. Haoyu Bai, Xingchuan He and Junjian Jin conducted the sample collection. Bijun Chen, Ziyi Li, Yaru Niu, Wen Yu and Shumin Du performed the experimental procedures and statistical analysis. Siriguleng Yu and Bijun Chen wrote and the manuscript text. All authors reviewed the manuscript.

**Acknowledgments.**- This study was supported by the National Natural Science Foundation of China (No. 32160821, 31860693). The contributions of Yuan Liu and Zhifang Xia from OBiO Technology (Shanghai) Corp., Ltd. (China) are acknowledged for their valuable input at the initial stages of the project.

**Conflict of interest statement.**- The authors declare that there are no conflicts of interest.

## REFERENCES

- Boussouar F. & Benahmed M. 2004. Lactate and energy metabolism in male germ cells. *J. Trends Endocrinol. Metab.* 15(7):345-350. <<https://dx.doi.org/10.1016/j.tem.2004.07.003>> <PMid:15350607>
- Chen X., Dong J. & Jiang Z.-Y. 2012. Nesfatin-1 influences the excitability of glucosensing neurons in the hypothalamic nuclei and inhibits the food intake. *Regul. Pept.* 177(1/3):21-26. <<https://dx.doi.org/10.1016/j.regpep.2012.04.003>> <PMid:22561448>
- Dong J., Guan H.-Z., Jiang Z.-Y. & Chen X. 2014. Nesfatin-1 influences the excitability of glucosensing neurons in the dorsal vagal complex and inhibits food intake. *PLoS One* 9(6):e98967. <<https://dx.doi.org/10.1371/journal.pone.0098967>> <PMid:24906120>
- Dong J., Xu H., Xu H., Wang P.-F., Cai G.-J., Song H.-F., Wang C.-C., Dong Z.-T., Ju Y.-J. & Jiang Z.-Y. 2013. Nesfatin-1 stimulates fatty-acid oxidation by activating AMP-activated protein kinase in STZ-induced type 2 diabetic mice. *PLoS One* 8(12):e83397. <<https://dx.doi.org/10.1371/journal.pone.0083397>> <PMid:24391760>
- Dore R., Levata L., Gachkar S., Jöhren O., Mittag J., Lehnert H. & Schulz C. 2017. The thermogenic effect of nesfatin-1 requires recruitment of the



- melanocortin system. *Endocrinology* 235(2):111-122. <<https://dx.doi.org/10.1530/JOE-17-0151>> <PMid:28851749>
- Foo K.S., Brauner H., Ostenson C.G. & Broberger C. 2010. Nucleobindin-2/nesfatin in the endocrine pancreas: distribution and relationship to glycaemic state. *Endocrinology* 204(3):255-263. <<https://dx.doi.org/10.1677/JOE-09-0254>> <PMid:20032201>
- Gantulga D., Maejima Y., Nakata M. & Yada T. 2012. Glucose and insulin induce Ca<sup>2+</sup> signaling in nesfatin-1 neurons in the hypothalamic paraventricular nucleus. *Biochem. Biophys. Res. Commun.* 420(4):811-815. <<https://dx.doi.org/10.1016/j.bbrc.2012.03.079>> <PMid:22465118>
- Gonzalez R., Reingold B.K., Gao X., Gaidhu M.P., Tsushima R.G. & Unniappan S. 2011. Nesfatin-1 exerts a direct, glucose-dependent insulinotropic action on mouse islet beta and MIN6 cells. *Endocrinology* 208(3):R9-R16. <<https://dx.doi.org/10.1530/JOE-10-0492>> <PMid:21224288>
- Li Q.-C., Wang H.-Y., Chen X., Guan H.-Z. & Jiang Z.-Y. 2010. Fasting plasma levels of nesfatin-1 in patients with type 1 and type 2 diabetes mellitus and the nutrient-related fluctuation of nesfatin-1 level in normal humans. *Regul. Pept.* 159(1/3):72-77. <<https://dx.doi.org/10.1016/j.regpep.2009.11.003>> <PMid:19896982>
- Li W., Li L., Wu Z., Liu J., Gong J., Liao H. & Liu X. 2018. Advances in chemical modification of proteins. *Chinese J. Cell Biol.* 40(10):1781-1786. <<https://dx.doi.org/10.11844/cjcb.2018.10.0104>>
- Li Z., Gao L., Tang H., Yin Y., Xiang X., Li Y., Zhao J., Mulholland M. & Zhang W. 2013. Peripheral effects of nesfatin-1 on glucose homeostasis. *J. PLoS One* 8(8):e71513. <<https://dx.doi.org/10.1371/journal.pone.0071513>> <PMid:23967220>
- Lim J., Park H.S., Kim J., Jang Y.J., Kim J.-H., Lee Y.J. & Heo Y. 2020. Depot-specific UCP1 expression in human white adipose tissue and its association with obesity-related markers. *Int. J. Obes.* 44(3):697-706. <<https://dx.doi.org/10.1038/s41366-020-0528-4>> <PMid:31965068>
- Oh-I S., Shimizu H., Satoh T., Okada S., Adachi S., Inoue K., Eguchi H., Yamamoto M., Imaki T., Hashimoto K., Tsuchiya T., Monden T., Horiguchi K., Yamada M. & Mori M. 2006. Identification of nesfatin-1 as a satiety molecule in the hypothalamus. *Nature* 443(7112):709-712. <<https://dx.doi.org/10.1038/nature05162>> <PMid:17036007>
- Ramanjaneya M., Chen J., Brown J.E., Tripathi G., Hallschmid M., Patel S., Kern W., Hillhouse E.W., Lehnert H., Tan B.K. & Randeve H.S. 2010. Identification of nesfatin-1 in human and murine adipose tissue: a novel depot-specific adipokine with increased levels in obesity. *Endocrinology* 151(7):3169-3180. <<https://dx.doi.org/10.1210/en.2009-1358>> <PMid:20427481>
- Ramesh N., Gawli K., Pasupuleti V.K. & Unniappan S. 2017. Metabolic and cardiovascular actions of nesfatin-1: implications in health and disease. *Curr. Pharm. Des.* 23(10):1453-1464. <<https://dx.doi.org/10.2174/1381612823666170130154407>> <PMid:28137218>
- Riva M., Nitert M.D., Voss U., Sathanoori R., Lindqvist A., Ling C. & Wierup N. 2011. Nesfatin-1 stimulates glucagon and insulin secretion and beta cell NUCB2 is reduced in human type 2 diabetic subjects. *Cell Tissue Res.* 346(3):393-405. <<https://dx.doi.org/10.1007/s00441-011-1268-5>> <PMid:22108805>
- Shimizu H., Oh-I S., Hashimoto K., Nakata M., Yamamoto S., Yoshida N., Eguchi H., Kato I., Inoue K., Satoh T., Okada S., Yamada M., Yada T. & Mori M. 2009. Peripheral administration of nesfatin-1 reduces food intake in mice: the leptin-independent mechanism. *Endocrinology* 150(2):662-671. <<https://dx.doi.org/10.1210/en.2008-0598>> <PMid:19176321>
- Tagaya Y., Osaki A., Miura A., Okada S., Ohshima K., Hashimoto K., Yamada M., Satoh T., Shimizu H. & Mori M. 2012. Secreted nucleobindin-2 inhibits 3T3-L1 adipocyte differentiation. *Protein Pept. Lett.* 19(9):997-1004. <<https://dx.doi.org/10.2174/092986612802084546>> <PMid:22486620>
- Yang G.-T., Zhao H.-Y., Kong Y., Sun N.-N. & Dong A.-Q. 2017. Study of the effects of nesfatin-1 on gastric function in obese rats. *World J. Gastroenterol.* 23(16):2940-2947. <<https://dx.doi.org/10.3748/wjg.v23.i16.2940>> <PMid:28522911>
- Yang Y., Zhang B., Nakata M., Nakae J., Mori M. & Yada T. 2019. Islet  $\beta$ -cell-produced NUCB2/nesfatin-1 maintains insulin secretion and glycemia along with suppressing UCP-2 in  $\beta$ -cells. *J. Physiol. Sci.* 69(5):733-739. <<https://dx.doi.org/10.1007/s12576-019-00689-2>> <PMid:31228099>
- Zhang Y., Lu J.-H., Zheng S.-Y., Yan J.-H., Chen L., Liu X., Wu W.-Z. & Wang F. 2017a. Serum levels of nesfatin-1 are increased in gestational diabetes mellitus. *Gynecol. Endocrinol.* 33(8):621-624. <<https://dx.doi.org/10.1080/09513590.2017.1306849>> <PMid:28361552>
- Zhang Y., Qu Y., Ma H.Y., Xu Y. & Dong J. 2017b. Effects and mechanisms of central nesfatin-1 on UCP-1 expression in adipose tissue. *Acta Acad. Med. Qingdao Universitatis* 53(6):631-639. <<https://dx.doi.org/10.13361/j.qdyxy.201706001>>
- Zhang Z., Li L., Yang M., Liu H., Boden G. & Yang G. 2012. Increased plasma levels of nesfatin-1 in patients with newly diagnosed type 2 diabetes mellitus. *Exp. Clin. Endocrinol. Diabetes* 120(02):91-95. <<https://dx.doi.org/10.1055/s-0031-1286339>> <PMid:22020667>